Vortex solitons in dipolar Bose-Einstein condensates

I. Tikhonenkov,[1] B. A. Malomed,[2] and A. Vardi[1]
[1]*Department of Chemistry, Ben-Gurion University of the Negev, P. O. Box 653, Beer-Sheva 84105, Israel*
[2]*Department of Physical Electronics, School of Electrical Engineering, Faculty of Engineering, Tel Aviv University, Tel Aviv 69978, Israel*
(Received 23 June 2008; published 28 October 2008)

We predict solitary vortices in quasiplanar condensates of dipolar atoms, polarized parallel to the confinement direction, with the effective sign of the dipole-dipole interaction inverted by means of a rapidly rotating field. Energy minima corresponding to vortex solitons with topological charges $\ell=1$ and 2 are predicted for moderately strong dipole-dipole interaction, using an axisymmetric Gaussian *Ansatz*. The stability of the solitons with $\ell=1$ is confirmed by full three-dimensional simulations, whereas their counterparts with $\ell=2$ are found to be unstable against splitting into a set of four fragments (quadrupole).

DOI: 10.1103/PhysRevA.78.043614 PACS number(s): 03.75.Lm, 05.30.Jp

I. INTRODUCTION

Matter-wave patterns in Bose-Einstein condensates (BECs) are sustained by the interplay between the external trapping potential and intrinsic interactions between atoms. In particular, bright solitons and soliton trains in nearly one-dimensional (1D) traps [1] are supported by the relatively weak attraction between atoms of ^{7}Li, or the stronger attraction in the ^{85}Rb condensate. For repulsive interactions, adding an axial optical-lattice (OL) potential gives rise to gap solitons, as demonstrated in ^{87}Rb [2].

In planar two-dimensional (2D) geometry with intrinsic repulsion, delocalized vortices constitute basic BEC patterns [3]. The creation of 2D matter-wave solitons (as well as 2D spatiotemporal solitons, alias "light bullets," in nonlinear optics [4]) is a challenge, as the contact attraction leads to collapse in this case. A square-shaped OL can stabilize fundamental solitons and solitary vortices (solitons with embedded vorticity) in two dimensions [5,6]. As concerns vortex solitons, the lattice breaks the isotropy of the embedding space and the related angular momentum conservation. Nevertheless, the intrinsic topological charge of the vortex can be defined unambiguously as $\ell \equiv \Delta\Phi/2\pi$, where $\Delta\Phi$ is the circulation of the phase of the corresponding complex wave function around the vortex pivot. The simplest "crater-shaped" vortices, in the form of a single density peak with an inner hole, trapped, essentially, in a single cell of the square lattice, are unstable [7]. Stable vortices with charge ℓ can be constructed, in the simplest form, as sets of four peaks, with phase shift $\Delta\varphi=\pi\ell/2$ between adjacent ones. Two stable four-peak vortex structures are possible, "rhombuses" (with a nearly empty cell in the middle) [5] and more compact "squares" [6]. For $\ell=2$, i.e., $\Delta\varphi=\pi$, these patterns are actually quadrupoles. Higher-order stable vortices, up to $\ell=6$, were found too, in the form of circular chains of 8 or 12 peaks [8]. Also found were "supervortices," built as ring-shaped chains of 12 compact (crater-shaped) local vortices with individual vorticity $l_0=1$, onto which global vorticity $\ell=\pm 1$ is imprinted [8]. The supervortex is stable despite the instability of crater-shaped vortices in isolation. Two-dimensional solitons, as well as vortices and quadrupoles of the rhombic type, can also be stabilized by quasi-1D OLs, i.e., periodic potentials depending on a single coordinate [9].

For repulsive contact interactions, a square-shaped OL can support 2D fundamental and vortical gap solitons [10]. In addition, axisymmetric radial potentials may stabilize solitons, including vortical ones, in both cases of attractive and repulsive interactions [11].

Despite the theoretical progress, 2D matter-wave solitons have not yet been observed, vortex solitons being a still more challenging subject. Therefore, the search for viable settings allowing the realization of such structures remains highly relevant. In parallel to BEC, theoretical and experimental studies of multidimensional spatiotemporal solitons draw great interest in nonlinear optics [4].

New possibilities for producing 2D solitons have emerged in dipolar quantum gases, such as BECs of magnetically polarized ^{52}Cr atoms [12], dipolar molecules [13], or atoms with electric moments induced by strong electric field [14] or laser illumination [15]. Of these systems, the gas of chromium atoms is the medium available for current experiments. For axisymmetric geometry, with dipoles polarized perpendicular to the 2D plane, the natural anisotropic dipole-dipole (DD) interaction gives rise to in-plane repulsion and axial attraction, which can support vortex lattices [16] and, in principle, 2D gap solitons (in the presence of the pertinent OL). On the other hand, the sign of the DD interaction may be reversed by means of rapid rotation of the dipoles [17] or by using a combination of microwave and dc fields [18], which enables the creation of isotropic solitons [19]. However, in the full three-dimensional (3D) geometry, isotropic vortex lines are destabilized by the DD interactions [20]. Alternatively, stable *anisotropic* solitons can be supported by the natural DD interaction, when dipoles are polarized in the 2D plane [21]. Related work in nonlinear optics employed the nonlocal thermal nonlinearity to predict stable vortex rings, with topological charges $\ell=1$ and 3 [22] and 2D elliptically shaped spatial solitons [23].

Here, we assume the axisymmetric configuration as in Ref. [19], with the aforementioned sign inversion of the DD interaction [17], to predict stable 2D vortex solitons. Families of vortex soliton states, with $\ell=1$ and 2, are constructed

in the framework of the 3D Gross-Pitaevskii (GP) equation, including the long-range DD interactions, contact repulsion, and transverse confinement potential. With topological charge $\ell=1$, the solitary vortex is stable, whereas the vortex soliton with $\ell=2$ splits via a quadrupole instability. Since the only reported experimental demonstration of 2D spatial vortex solitons requires the presence of photonic lattices in photorefractive crystals [25], and because no observation of vortex solitons was reported in uniform media, the proposal to create such solitons in dipolar BECs is pertinent to the experiment, especially in view of recent advances in tuning out the local nonlinearity via a Feshbach resonance (FR) [24].

The paper is organized as follows. In Sec. I, we apply a variational approximation to predict localized-vortex states yielding a minimum of the dipolar condensate energy. Naturally, these states have a chance to represent stable vortex solitons. In Sec. III, results of direct simulations of vortex solitons, performed in the framework of the full 3D GP equation, are summarized. For that purpose, we use both numerically exact profiles, which are generated from the variational *Ansätze* by means of the preliminarily simulated propagation in imaginary time, and the *Ansätze* themselves, the corresponding results being quite similar. The paper is concluded by Sec. IV. In particular, in that section we discuss the physical significance of three-body losses induced by the FR.

II. VARIATIONAL ANALYSIS FOR ENERGY MINIMA

We assume that a strong magnetic field aligns dipole moments along the confinement axis z [17–19]. The corresponding GP energy functional, expressed in terms of the BEC order parameter $\psi(x,y,z)$, is

$$E\{\psi\}=T+V+U+U_d, \tag{1}$$

where the kinetic, confinement, and contact-interaction energies are, respectively,

$$T=\frac{1}{2}\int|\nabla\psi(\mathbf{r})|^2d\mathbf{r},\quad V=\frac{1}{2}\int z^2|\psi(\mathbf{r})|^2d\mathbf{r}, \tag{2}$$

$$U=\frac{g}{2}\int|\psi(\mathbf{r})|^4d\mathbf{r}, \tag{3}$$

and the DD mean-field energy is

$$U_d=\frac{g_d}{2}\iint\left(1-\frac{3(z-z')^2}{|\mathbf{r}-\mathbf{r}'|^2}\right)|\psi(\mathbf{r}')|^2|\psi(\mathbf{r})|^2\frac{d\mathbf{r}\,d\mathbf{r}'}{|\mathbf{r}-\mathbf{r}'|^3}. \tag{4}$$

Here and below, the length, time, and energy are scaled as $\mathbf{r}\to\mathbf{r}/l_z$, $t\to\omega_z t$, and $E\to E/(\hbar\omega_z)$, where ω_z is the transverse trap frequency and $l_z\equiv\sqrt{\hbar/m\omega_z}$ is its length. The interaction strengths are $g=4\pi Na_s/l_z$ and $g_d=Nd^2m(\hbar^2l_z)^{-1}$, where $a_s>0$ is the s-wave scattering length, d and m the atomic dipole moment and mass, N the number of atoms, and the normalization is taken in the form of $\int|\psi(\mathbf{r})|^2d\mathbf{r}=1$.

To approximate vortex-soliton states with topological charge ℓ, we use the normalized Gaussian *Ansatz* in cylindrical coordinates z, $\rho\equiv\sqrt{x^2+y^2}$, and $\phi\equiv\tan^{-1}(y/x)$,

$$\psi_\ell(\rho,z,\phi)=A_\ell\rho^\ell\exp[-(\alpha\rho^2+\gamma z^2)/2]\exp(i\ell\phi), \tag{5}$$

where $A_\ell^2=(\pi^{-3/2}/\ell)\alpha^{\ell+1}\gamma^{1/2}$ for $\ell=1,2$. Evaluating $E\{\psi_\ell\}$, we obtain

$$E\{\psi_1\}=\alpha+\frac{1}{4}\left(\gamma+\frac{1}{\gamma}\right)+\frac{1}{2}\alpha\sqrt{\frac{\gamma}{2\pi}}\left(\frac{g}{4\pi}+\frac{g_d}{3}f_1(\kappa)\right), \tag{6}$$

$$E\{\psi_2\}=\frac{3}{2}\alpha+\frac{1}{4}\left(\gamma+\frac{1}{\gamma}\right)+\frac{3}{8}\alpha\sqrt{\frac{\gamma}{2\pi}}\left(\frac{g}{4\pi}+\frac{g_d}{3}f_2(\kappa)\right), \tag{7}$$

where the functions

$$f_1(\kappa)=-1+3\int_0^1R(\kappa,x)[1+Q^2(\kappa,x)]dx,$$

$$f_2(\kappa)=-1+3\int_0^1R(\kappa,x)\left(1+\frac{2}{3}Q^2(\kappa,x)+Q^4(\kappa,x)\right)dx,$$

$$R(\kappa,x)\equiv\frac{(\kappa x)^2}{(\kappa x)^2+(1-x^2)},\quad Q(\kappa,x)\equiv\frac{1-x^2}{(\kappa x)^2+(1-x^2)} \tag{8}$$

depend solely on the *aspect ratio* $\kappa\equiv\sqrt{\gamma/\alpha}$.

In strongly prolate (cigar-shaped) geometry with $\kappa\ll1$, one has $R\to0$, $Q\to1$, and $f_{1,2}(\kappa)\to-1$. By contrast, for an oblate (pancake) shape with $\kappa\gg1$, we have $R\to1$, $Q\to0$, and $f_{1,2}(\kappa)\to2$. The change of the sign of $f_{1,2}$ with the transition from $\kappa\ll1$ to $\kappa\gg1$ is due to the corresponding change of the relative strength of "side-by-side" and "head-to-tail" DD interactions, which dominate the prolate and oblate configurations, respectively. Consequently, for $g_d>0$ and fixed γ, the integrated DD energy U_d *decreases* both for $\alpha\to0$ (since $U_d>0$ for large κ) and $\alpha\to\infty$ (because $U_d<0$ in this limit), leading to either expansion or collapse along ρ.

Inversion of the sign of g_d [17–19] converts the energy maximum at the prolate-oblate transition point into a minimum. It is thus required to stabilize 2D isotropic patterns, with the dipolar moments polarized along the cylindrical axis. This requirement for g_d inversion, in combination with the necessity to reduce the strong contact repulsion using the FR, is an experimental challenge. The existence of stable *anisotropic* fundamental (nontopological) solitons, with the dipoles polarized in the (x,y) plane and the ordinary sign of the DD interaction ($g_d>0$) [21], suggests that anisotropic topological (vortexlike) solitons may be found in the same setting. However, we leave the analysis of such complex patterns to a separate work, aiming here to retain the cylindrical symmetry, adopting the assumption of $g_d<0$.

Assuming the sign inversion of the DD interaction, the minimum in U_d as a function of α at $\gamma\sim1$ will translate into a minimum of total energy E, provided that U_d is large enough to offset the contact-interaction and gradient terms U and T, both scaling linearly with α. This requirement results in the necessary condition for the existence of a stable isotropic vortex soliton,

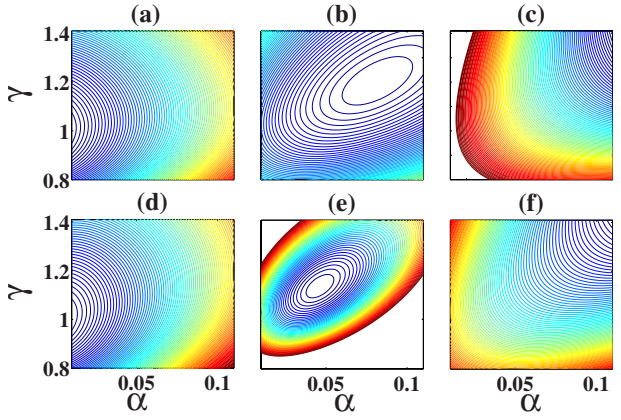

FIG. 1. (Color online) GP energy functional for the vortex-soliton *Ansatz* (5), with $\ell=1$ (a)–(c) and 2 (d)–(f), as a function of variational parameters α and γ. In all plots, $g=20$, with $g_d=-10$ (a), -20 (b), -30 (c) for $\ell=1$, and $g_d=-20$ (d), -30 (e), -40 (f) for $\ell=2$.

$$g_d < 6\sqrt{2\pi}\ell + 3g/(4\pi) < -2g_d. \tag{9}$$

The inequalities on the right- and left-hand sides of Eq. (9) guarantee, severally, $\partial E(\alpha,\gamma)/\partial\alpha<0$ for $\alpha\to 0$ ($f_\ell\to 2$) and $\partial E(\alpha,\gamma)/\partial\alpha>0$ for $\alpha\to\infty$ ($f_\ell\to -1$). As expected, the conditions (9) can be satisfied only for $g_d<0$. The required strength $|g_d|$ increases with ℓ due to the growing centrifugal contribution to the kinetic energy, which must be balanced by the attractive part of the DD interaction. In the strong-interaction regime, with $3g/4\pi \gg 6\sqrt{2\pi}\ell$, the kinetic term may be neglected, and Eq. (9) simplifies to $-g_d/g>3/(8\pi)$.

Condition (9) only guarantees a minimum of the GP energy as a function of α for fixed γ, which is not yet sufficient for a true minimum of $E(\alpha,\gamma)$ in the (α,γ) plane. In particular, fixing κ and varying $\gamma=\kappa^2\alpha$, one can see that $U+U_d \propto \gamma^{3/2}$, $V\propto 1/\gamma$, and $T\propto\gamma$, so that the kinetic energy T cannot balance the interaction terms $U+U_d$ for large γ. Since $U+U_d<0$ in the large-κ sector of the (α,γ) plane, this will lead to 3D collapse, with α, $\gamma\to\infty$, *unless* the vertical confinement size l_z is smaller than the effective healing length, determined by the interplay of the kinetic energy with the combined contact and DD interactions.

In Fig. 1, we plot the GP energies, as given by Eq. (6) [Figs. 1(a)–1(c)] and Eq. (7) [Figs. 1(d)–1(f)], in three characteristic interaction-parameter regimes. For $\ell=1$ and 2, respectively, Figs. 1(a) and 1(d) display cases when the DD interaction is too weak to satisfy conditions (9). This results in a monotonic decrease of the energy as $\alpha\to 0$ at fixed γ, causing the radial expansion of the BEC. On the other hand, if the DD interaction is too strong, the energy decreases monotonically for fixed κ as α, $\gamma\to\infty$, implying the 3D collapse [Figs. 1(c) and 1(f)]. In the intermediate regime, the DD interaction is strong enough to offset the dispersive effect of the contact and kinetic terms, yet is not so excessively strong as to induce the 3D collapse. This regime gives rise to local energy minima, which are found at $g=-g_d=20$ for $\alpha=0.081$, $\gamma=1.15$ in Fig. 1(b), and at $g=20$, $g_c=-30$ for $\alpha=0.046$, $\gamma=1.13$ in Fig. 1(e). These minima suggest the possibility of metastable oblate vortex solitons, with radial widths of $3.51l_z$ and $4.66l_z$ for $\ell=1,2$ respectively.

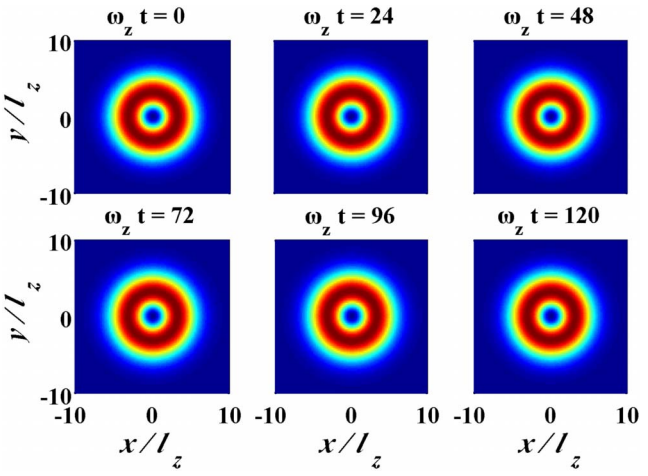

FIG. 2. (Color online) Evolution of a vortex soliton with $\ell=1$, for $g=-g_d=20$. The initial conditions are obtained by imaginary-time propagation for $i\omega_z t=30$, starting from the Gaussian *Ansatz* (5) with $\alpha=0.08$ and $\gamma=1.15$, which corresponds to the energy minimum in Fig. 1(b). The evolution of the density profile in cross section $z=0$ demonstrates the stability of the solitary vortex with $\ell=1$.

III. MEAN-FIELD DYNAMICS AND STABILITY

To directly verify the existence and stability of axisymmetric vortex solitons, we substituted the values of α and γ corresponding to the local energy minima into *Ansatz* (5), and simulated its evolution according to the full time-dependent GP equation,

$$i\frac{\partial}{\partial t}\psi = \left[-\frac{1}{2}\nabla^2+\frac{1}{2}z^2+g|\psi|^2+g_d\int\left(1-\frac{3(z-z')^2}{|\mathbf{r}-\mathbf{r}'|^2}\right)\times|\psi(\mathbf{r}')|^2\frac{d\mathbf{r}'}{|\mathbf{r}-\mathbf{r}'|^3}\right]\psi. \tag{10}$$

First, propagation in imaginary time was carried out to reshape the input into a numerically exact stationary solitary vortex. The amplitude difference between the initial Gaussian *Ansatz* and the reshaped soliton was less than 10%. Then, to test the stability of the solitary vortices, we used these profiles as initial conditions and carried out 3D simulations in real time. The local density and phase at $z=0$, during real-time evolution for approximately 20 trap periods, are shown in Figs. 2 and 3 for $\ell=1$, and in Figs. 4 and 5 for $\ell=2$. With topological charge $\ell=1$, the vortex soliton remains virtually unchanged during the evolution (Fig. 2), which demonstrates its full stability. By contrast, with $\ell=2$, the solitary vortex is modulationally unstable against splitting into a quadrupole set, as shown in Fig. 4. This observation is reminiscent of the stability analysis for solitary vortices in condensates with local self-attraction, trapped in an axisymmetric parabolic potential [26], where only $\ell=1$ vortices have a stability region, all vortices with $\ell>1$ being inherently unstable.

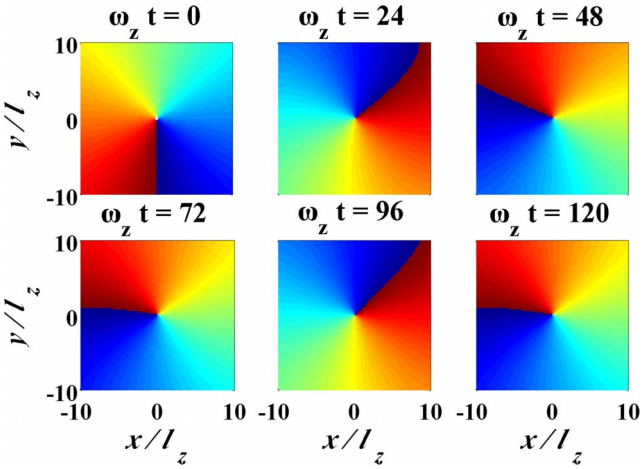

FIG. 3. (Color online) Phase plots during the evolution of the solitary vortex with $\ell=1$ and the same parameters as in Fig. 2.

The evolution of the solitary vortex with $\ell=1$ was also compared to the GP dynamics in limiting cases when either the contact repulsion or DD interaction is turned off. As mentioned above, the contact interaction may be experimentally controlled by means of the FR [24], and the DD interaction may be tuned using additional external fields [17,18], or simply turned off by removing the polarizing field, which allows the dipolar order to be frustrated. In Figs. 6(a)–6(c), we display the density and phase distributions in cross section $z=0$, for $\ell=1$ and $\omega_z t=12$. Recall that the vortex soliton was robust for unaltered interaction strengths [Fig. 6(a)]. In contrast to that, when the DD interaction is turned off [Fig. 6(b)], radial expansion is observed, accompanied by an outgoing density current. On the other hand, when the g_d/g ratio is too large, the vortex collapses [see Fig. 6(c)], and the current is funneled toward the vertical axis. It is noteworthy that the axial symmetry is maintained in all cases.

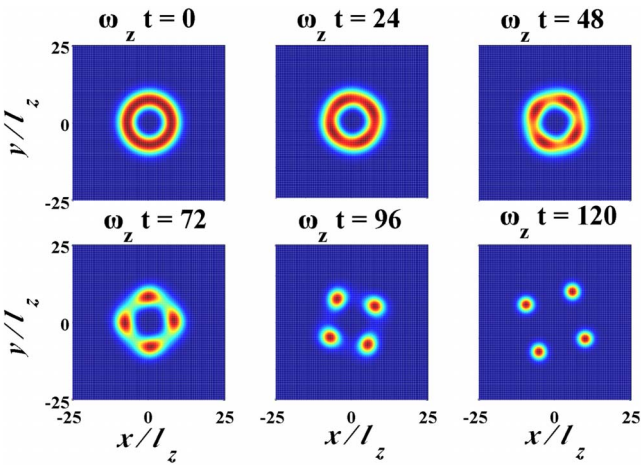

FIG. 4. (Color online) Evolution of the density profile in cross section $z=0$ for a vortex soliton with $\ell=2$ and interaction strengths $g=20$, $g_d=-30$. Initial conditions were generated by imaginary-time propagation for $i\omega_z t=30$, starting from the Gaussian *Ansatz* (5) with $\ell=2$, $\alpha=0.046$, $\gamma=1.13$, which corresponds to the energy minimum in Fig. 1(e). The solitary vortex is unstable, and eventually splits into a quadrupole set.

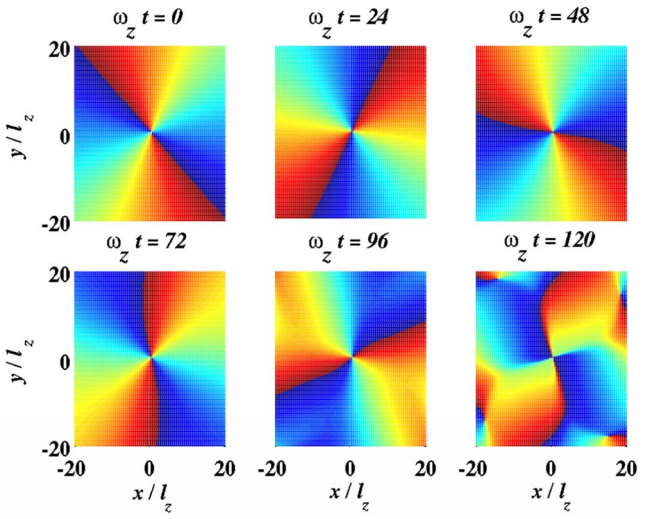

FIG. 5. (Color online) Phase plots during the evolution of the solitary vortex with $\ell=2$ and the same parameters as in Fig. 4.

The stability of the solitary vortex with $\ell=1$ is further corroborated by the simulated propagation in real time of the initial configuration corresponding to the Gaussian *Ansatz* (5), with α and γ set to the location of the minimum in Fig. 1(b). This state, which actually corresponds to a slightly perturbed vortex soliton, demonstrates, for $g=-g_d=20$, stable self-trapping into the exact solitary vortex [Fig. 6(d)]. By contrast, expansion [Fig. 6(e)] and collapse [Fig. 6(f)] are

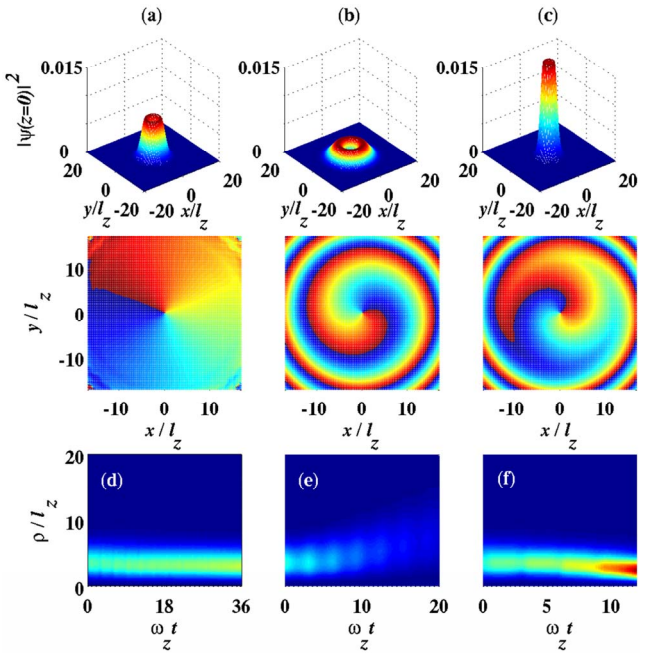

FIG. 6. (Color online) Density profiles (first row) and phase plots (second row) in cross section $z=0$, after real-time propagation for $\omega_z t=12$, starting from the vortex-soliton state with $\ell=1$, as taken from Fig. 2. The robust evolution of the solitary vortex for $g=-g_d=20$ (a) is compared to the expansion for $g=20$, $g_d=0$ (b) and collapse for $g=0$, $g_d=-20$ (c). (d)–(f) show the real-time evolution of the density profile $|\psi(\rho,z=0,\phi)|^2$, starting with the approximate Gaussian *Ansatz* (5), for the same parameters.

observed, respectively, in the regimes of too weak [as in Fig. 1(a)] and too strong [Fig. 1(c)] DD interactions.

IV. CONCLUSIONS

The experimental feasibility of quasi-2D solitons in dipolar BECs was estimated in Refs. [19,21]. For ^{52}Cr atoms, the natural DD to contact interaction strength ratio is less than 0.1 [12]. Therefore, essential attenuation of the contact interaction by means of the FR is necessary [24]. One consequence of this requirement to the experiment is that three-body losses, which are also induced by the FR, of order 10^{-28} cm^6 s^{-1} [27], will set an upper limit on the free-evolution time and impose an intrinsic time dependence. Preliminary numerical simulations including a quintic loss term of this magnitude indicate that soliton behavior is not considerably affected by these losses. The remaining difficulty (as for the fundamental solitons predicted in Ref. [19]) is the necessity to invert the sign of the DD interaction by means of a rapidly rotating magnetic field [17], a technique which still has to be experimentally demonstrated.

In conclusion, using variational analysis and direct simulations of the GP equation in three dimensions, we have predicted the existence of stable quasi-2D vortex solitons with topological charge $\ell=1$ in a dipolar BEC with atomic moments polarized perpendicular to the 2D plane, and inverted sign of the dipole-dipole interaction. While energy minima exist also for solitary vortices with $\ell=2$, the resulting soliton is unstable and splits into a quadrupole set after the evolution in the course of a few trap periods. Future work will explore the possibility of anisotropic solitary vortices with an in-plane polarization axis and the natural sign of the DD interactions.

ACKNOWLEDGMENTS

We appreciate valuable discussions with T. Pfau. This work was supported by the Israel Science Foundation (Grant No. 582/07).

[1] K. E. Strecker, G. B. Partridge, A. G. Truscott, and R. G. Hulet, Nature (London) **417**, 150 (2002); L. Khaykovich, F. Schreck, G. Ferrari, T. Bourdel, J. Cubizolles, L. D. Carr, Y. Castin, and C. Salomon, Science **296**, 1290 (2002); S. L. Cornish, S. T. Thompson, and C. E. Wieman, Phys. Rev. Lett. **96**, 170401 (2006).

[2] B. Eiermann, Th. Anker, M. Albiez, M. Taglieber, P. Treutlein, K.-P. Marzlin, and M. K. Oberthaler, Phys. Rev. Lett. **92**, 230401 (2004).

[3] M. R. Matthews, B. P. Anderson, P. C. Haljan, D. S. Hall, C. E. Wieman, and E. A. Cornell, Phys. Rev. Lett. **83**, 2498 (1999); A. L. Fetter and A. A. Svidzinsky, J. Phys. Condens. Matter **13**, R135 (2001); P. Engels, I. Coddington, V. Schweikhard, and E. A. Cornell, J. Low Temp. Phys. **134**, 683 (2004).

[4] B. A. Malomed, D. Mihalache, F. Wise, and L. Torner, J. Opt. B: Quantum Semiclassical Opt. **7**, R53 (2005).

[5] B. B. Baizakov, B. A. Malomed, and M. Salerno, Europhys. Lett. **63**, 642 (2003).

[6] J. Yang and Z. H. Musslimani, Opt. Lett. **28**, 2094 (2003); Z. H. Musslimani and J. Yang, J. Opt. Soc. Am. B **21**, 973 (2004).

[7] R. Driben, B. A. Malomed, A. Gubeskys, and J. Zyss, Phys. Rev. E **76**, 066604 (2007).

[8] H. Sakaguchi and B. A. Malomed, Europhys. Lett. **72**, 698 (2005).

[9] B. B. Baizakov, B. A. Malomed, and M. Salerno, Phys. Rev. A **70**, 053613 (2004); T. Mayteevarunyoo, B. A. Malomed, B. B. Baizakov, and M. Salerno, Physica D (to be published).

[10] B. B. Baizakov, V. V. Konotop, and M. Salerno, J. Phys. B **35**, 5105 (2002); E. A. Ostrovskaya and Yu. S. Kivshar, Phys. Rev. Lett. **90**, 160407 (2003); **93**, 160405 (2004); H. Sakaguchi and B. A. Malomed, J. Phys. B **37**, 2225 (2004).

[11] Y. V. Kartashov, V. A. Vysloukh, and L. Torner, Phys. Rev. Lett. **93**, 093904 (2004); **94**, 043902 (2005); B. B. Baizakov, B. A. Malomed, and M. Salerno, Phys. Rev. E **74**, 066615 (2006).

[12] A. Griesmaier, J. Werner, S. Hensler, J. Stuhler, and T. Pfau, Phys. Rev. Lett. **94**, 160401 (2005); J. Stuhler, A. Griesmaier, T. Koch, M. Fattori, T. Pfau, S. Giovanazzi, P. Pedri, and L. Santos, *ibid.* **95**, 150406 (2005); J. Werner, A. Griesmaier, S. Hensler, J. Stuhler, T. Pfau, A. Simoni, and E. Tiesinga, *ibid.* **94**, 183201 (2005); A. Griesmaier, J. Stuhler, T. Koch, M. Fattori, T. Pfau, and S. Giovanazzi, *ibid.* **97**, 250402 (2006); A. Griesmaier, J. Phys. B **40**, R91 (2007); T. Lahaye, T. Koch, B. Fröhlich, M. Fattori, J. Metz, A. Griesmaier, S. Giovanazzi, and T. Pfau, Nature (London) **448**, 672 (2007).

[13] T. Köhler, K. Góral, and P. S. Julienne, Rev. Mod. Phys. **78**, 1311 (2006); J. M. Sage, S. Sainis, T. Bergeman, and D. DeMille, Phys. Rev. Lett. **94**, 203001 (2005); C. Ospelkaus, S. Ospelkaus, L. Humbert, P. Ernst, K. Sengstock, and K. Bongs, *ibid.* **97**, 120402 (2006).

[14] M. Marinescu and L. You, Phys. Rev. Lett. **81**, 4596 (1998).

[15] S. Giovanazzi, D. O'Dell, and G. Kurizki, Phys. Rev. Lett. **88**, 130402 (2002); I. E. Mazets, D. H. J. O'Dell, G. Kurizki, N. Davidson, and W. P. Schleich, J. Phys. B **37**, S155 (2004); R. Löw, R. Gati, J. Stuhler, and T. Pfau, Europhys. Lett. **71**, 214 (2005).

[16] S. Yi and H. Pu, Phys. Rev. A **73**, 061602(R) (2006); V. M. Lashkin, *ibid.* **75**, 043607 (2007).

[17] S. Giovanazzi, A. Görlitz, and T. Pfau, Phys. Rev. Lett. **89**, 130401 (2002).

[18] A. Micheli, G. Pupillo, H. P. Büchler, and P. Zoller, Phys. Rev. A **76**, 043604 (2007).

[19] P. Pedri and L. Santos, Phys. Rev. Lett. **95**, 200404 (2005); R. Nath, P. Pedri, and L. Santos, Phys. Rev. A **76**, 013606 (2007).

[20] M. Klawunn, R. Nath, P. Pedri, and L. Santos, Phys. Rev. Lett. **100**, 240403 (2008).

[21] I. Tikhonenkov, B. A. Malomed, and A. Vardi, Phys. Rev. Lett. **100**, 090406 (2008).

[22] D. Briedis, D. E. Petersen, D. Edmundson, W. Królikowski,

and O. Bang, Opt. Express **13**, 435 (2005); S. Skupin, O. Bang, D. Edmundson, and W. Królikowski, Phys. Rev. E **73**, 066603 (2006).

[23] C. Rotschild, O. Cohen, O. Manela, M. Segev, and T. Carmon, Phys. Rev. Lett. **95**, 213904 (2005).

[24] T. Koch, T. Lahaye, J. Metz, B. Frölich, A. Griesmaier, and T. Pfau, Nat. Phys. **4**, 218 (2008).

[25] D. N. Neshev, T. J. Alexander, E. A. Ostrovskaya, Y. S. Kivshar, H. Martin, I. Makasyuk, and Z. Chen, Phys. Rev. Lett. **92**, 123903 (2004); J. W. Fleischer, G. Bartal, O. Cohen, O. Manela, M. Segev, J. Hudock, and D. N. Christodoulides, *ibid.* **92**, 123904 (2004).

[26] T. J. Alexander and L. Bergé, Phys. Rev. E **65**, 026611 (2002); D. Mihalache, D. Mazilu, B. A. Malomed, and F. Lederer, Phys. Rev. A **73**, 043615 (2006).

[27] T. Pfau (private communication).